Abstract:	This memorandum takes a look at some of the history behind the well-known Gaussian probability density function (PDF). The summation of independent random variables (IRV) is specifically examined as a means to approximate the Gaussian PDF. Numerical methods are exploited to investigate the Gaussian PDF's connection with other known concepts that arise in electrical engineering.
Date:	23 February 2005
Author:	J.A. Crawford
Reference No.	U11685

1 Introduction

This memorandum seeks to look at the Gaussian distribution in a number of ways that have not necessarily found their way into the main-stream media. This memorandum is written from an engineering perspective rather than a mathematical or statistical perspective, and ample use of numerical tools and techniques are used to illustrate different points throughout the paper.

The main emphasis of this memorandum examines the viability of using a sum of independent random variables (IRV) to approximate the Gaussian distribution. Although the Central Limit Theorem predicts that a Gaussian PDF results in the limit as an infinite number of IRVs are summed, it is very interesting to examine this question for a finite number n of summed IRVs.

2 Some History

A short history of the Gaussian distribution and how it received is name can be found in [9]. This same reference provides three historically important derivations of the Gaussian PDF: (i) Herschel-Maxwell, (ii) Gauss derivation based upon maximum-likelihood, and (iii) Landon. Each of these derivations is worthy of some familiarity because they provide insights that can otherwise be missed.

3 Sum of Uniformly Distributed Random Variables

It is well known that the sum of a set of uniformly distributed independent random variables (URV) exhibits an increasingly Gaussian PDF as the number of variables summed increases. In this section, we will look at the relationship between the resultant distribution of the sum, and the number of variables used in the summation, n. We will also show that as $n \rightarrow \infty$, the probability density does in fact become Gaussian. We will be primarily interested in the behavior of the probability tails of the distributions involved.

In the case of two summed URV's, the resultant PDF is of course triangular in shape (See Figure 2). Larger values of n result in more complicated shapes that are increasingly Gaussian in shape (See Figure 2 through Figure 4). The question regarding the similarity of the summed URV PDF with that of the ideal Gaussian PDF versus n remains to be addressed.

A URV over the range [-1/2, 1/2] is shown in Figure 1. The total area must equal unity which results in the density having unit-height across the span of the distribution.

Figure 1 Simple Uniformly Distributed RV

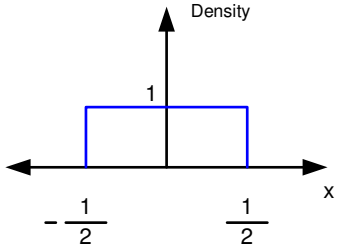

The characteristic function is a very powerful tool that is well suited for the study of IRV sums and it will be employed throughout this memorandum. Although other techniques can be used to arrive at the same results provided in this memorandum, the characteristic function methods employed herein are by far the more simple and most engineering-centric. Additional information regarding characteristic functions can be found in Section 7.1.

The characteristic function for the single URV is given by

$$\textbf{(1)} \quad C_1(f) = \frac{\sin(\pi f)}{\pi f}$$

and is nothing more than a Fourier transform of the underlying PDF. By definition, the variance of a URV is

(2) $$\sigma_u^2 = \int_{-1/2}^{1/2} x^2 dx = \frac{1}{12}$$

If n such URVs are summed, the variance would increase linearly with n as n/12 if the distribution in Figure 1 is used unchanged. In order to keep the variance of the sum of n URVs constant (i.e., 1/12), the probability density function in Figure 1 must be modified such that its extent on the x-axis varies with n as [-1/(2√n), 1/(2√n)], and its height varies as √n. The characteristic function for a single URV meeting these requirements is given by

(3) $$C_{n1}(f) = \frac{\sin\left(\frac{\pi f}{\sqrt{n}}\right)}{\left(\frac{\pi f}{\sqrt{n}}\right)}$$

and the corresponding characteristic function for the sum of n such URVs is given by

(4) $$C_n(f,n) = \left[\frac{\sin\left(\frac{\pi f}{\sqrt{n}}\right)}{\left(\frac{\pi f}{\sqrt{n}}\right)}\right]^n$$

Figure 2 PDFs for the Sum of Uniformly Distributed RV's

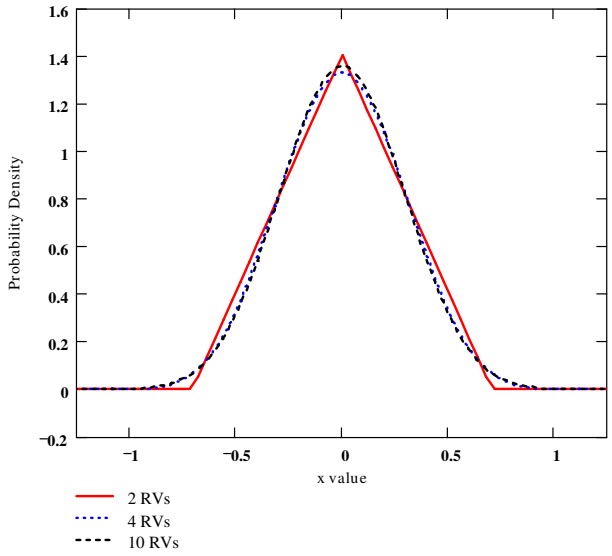

Figure 3 Repeat of Figure 2 But With Log Y-Axis Scale (Numerical Precision Limits Appearing for n=2 Case)

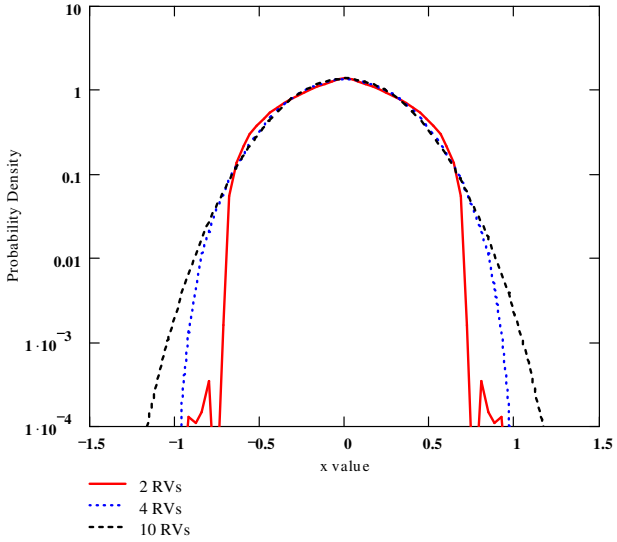

Figure 4 PDF for Uniformly Distributed RV Suitable for Use with Sums of 1,4, and 6 RVs

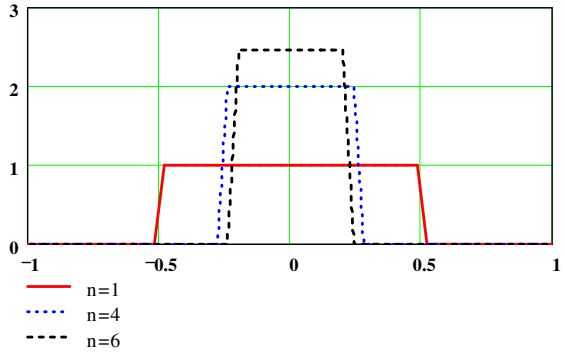

As shown in Figure 4, the PDFs become higher and narrower as n increases.

The resultant characteristic functions are shown from (4) for n= 1, 2, 8 and 50 in Figure 5. The curves for n=8 and n=50 almost lie on top of each other making it difficult to resolve them individually in the figure. Based upon this figure, it may seem likely to assume that perhaps a sum of 50 URVs is adequate to closely approximate a true Gaussian PDF, but as we will see shortly, this conclusion may be premature depending upon the judgment criteria adopted. As shown in Figure 6, the shape of the characteristic function is still changing even for n= 500.

Figure 5 Characteristic Functions for n= 1, 2, 8 and 50 (Positive x-Axis Portion Only)

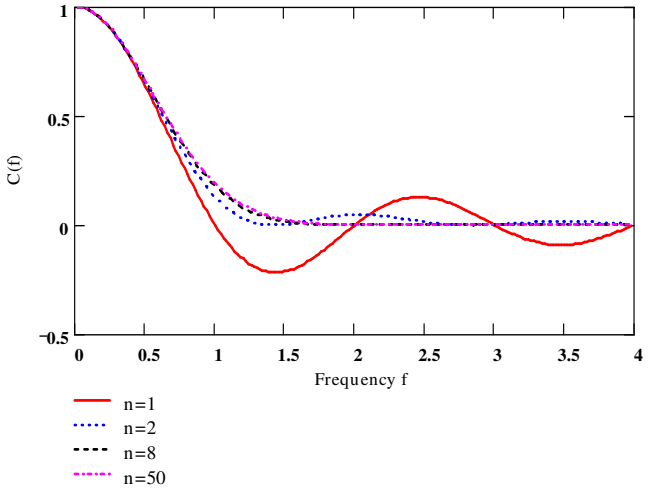

From Figure 6, it is apparent that the shape of the characteristic function is approaching an asymptotic limit as n increases. This is indeed true.

Figure 6 Characteristic Functions for Uniform RV Sum (Similar to Figure 5 Except Log Scale for Y-Axis)

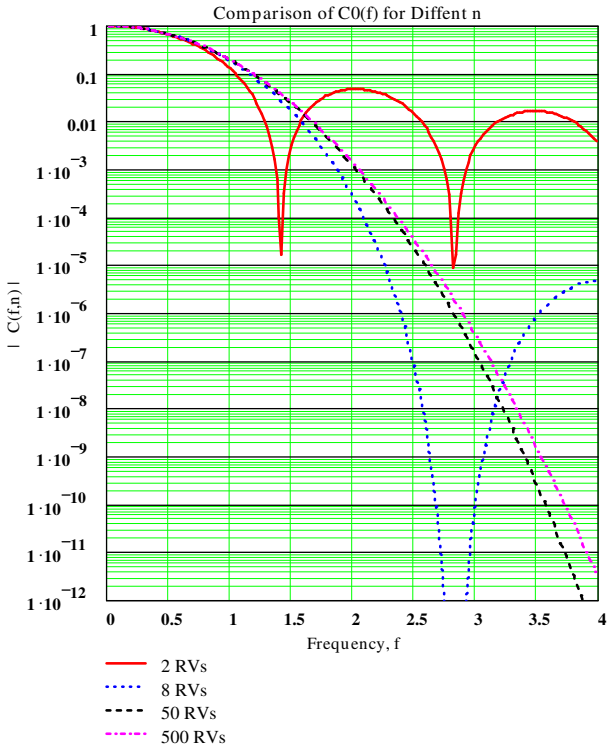

Since there is a one-to-one relationship between a PDF and its characteristic function, it is worthwhile to investigate the behavior of equation (4) as n → ∞. If the resulting characteristic function in the limit equals the characteristic function of an ideal Gaussian RV, we will in fact have shown that an infinite sum of URVs is in fact Gaussian. Pursuing this path further, we can first make use of the Taylor series expansion for the sine function in (4) to write

$$\textbf{(5)}\quad \frac{\sin(x)}{x} = \frac{x - \frac{x^3}{3!} + \frac{x^5}{5!} - \frac{x^7}{7!} \pm \ldots}{x} \approx 1 - \frac{x^2}{6}$$

where only the first two terms of the expansion have been retained and x= πf / √n. The binomial expansion formula can be used next to expand the exponentiation portion in equation (4) as

$$\textbf{(6)}\quad (1-\alpha)^n = 1 - n\alpha + \frac{n(n-1)\alpha^2}{2} - \frac{n(n-1)(n-2)\alpha^3}{3!} + \frac{n(n-1)(n-2)(n-3)\alpha^4}{4!} \mp \ldots$$

in which α= (πf)^2 / (6n). Once α is substituted into (6), we obtain the more interesting result

$$\textbf{(7)}\quad (1-\alpha)^n = 1 - n\frac{u}{n} + \frac{n(n-1)}{2!}\frac{u^2}{n^2} - \frac{n(n-1)(n-2)}{3!}\frac{u^3}{n^3} \pm \ldots$$

where u= (πf)^2/6. In this form, it is clear how the role of n is eliminated as n → ∞ with the numerator and the denominator "n-terms" canceling out. In the limit, we may subsequently write

$$\textbf{(8)}\quad \lim_{n\to\infty}(1-\alpha)^n = 1 + \sum_{k=1}^{\infty}\frac{1}{k!}\left[-\frac{(\pi f)^2}{6}\right]^k$$

This result is unmistakable recalling that the Taylor series expansion for a simple exponential is given by

$$\textbf{(9)}\quad e^x = 1 + x + \frac{x^2}{2!} + \frac{x^3}{3!} + \ldots = 1 + \sum_{k=1}^{\infty}\frac{x^k}{k!}$$

We can subsequently conclude that

$$\textbf{(10)}\quad \lim_{n\to\infty}\left[\frac{\sin\left(\frac{\pi f}{\sqrt{n}}\right)}{\left(\frac{\pi f}{\sqrt{n}}\right)}\right]^n = e^{-\frac{\pi^2}{6}f^2} = e^{-\frac{1}{2}(\sigma 2\pi f)^2}$$

where $\sigma^2 = 1/12$ as we started out with. The right-hand side of (10) is the well-known characteristic function for an ideal Gaussian RV. Since the characteristic function of the URV sum equals the characteristic function of the ideal Gaussian in the limit as $n \to \infty$, we can conclude that the sum does in fact become asymptotically Gaussian.

Even though the Central Limit Theorem of probability theory clearly predicts that the URV sum will become Gaussian in the limit, this is nonetheless an intriguing and exciting result. For one thing, the result shows that the truncation of the characteristic function details beyond the first two terms retained in (5) does not matter. Intuitively, it is therefore very plausible that the shape of the RV's PDF being summed probably does not matter significantly either, which is again another conclusion that the Central Limit Theorem would predict. We will take a short look at this aspect of summing RV with other density functions in Section 4.

3.1 Uniformly Distributed RVs: How Many?

We know from the preceding discussion that the sum of URVs becomes Gaussian in the limit as $n \to \infty$. It is interesting however to look at the behavior of the resulting PDF when a finite number of URVs are used in the summation.

Since the variance of a sum of independent URVs is equal to the sum of their individual variances, there is no mystery regarding the behavior of the variance with n. The behavior of the probability tails is however of considerable interest, particularly for any work involving the modeling of Gaussian noise. The PDF of the sum is most easily computed by using the inverse of the characteristic function (4) as

$$\textbf{(11)}\quad pdf\,(x,n) = \int_{-\infty}^{+\infty} \left[\frac{\sin\left(\frac{\pi f}{\sqrt{n}}\right)}{\left(\frac{\pi f}{\sqrt{n}}\right)} \right]^n e^{-j2\pi fx} df$$

The tail probability for the sum on n URVs can be computed as

$$P(\lambda) = \int_{\lambda}^{\infty} pdf\,(x,n)\,dx$$

$$\textbf{(12)}\quad = \int_{\lambda}^{\infty} dx \int_{-\infty}^{+\infty} df \left[\frac{\sin\left(\frac{\pi f}{\sqrt{n}}\right)}{\left(\frac{\pi f}{\sqrt{n}}\right)} \right]^n e^{-j2\pi fx}$$

for $\lambda \geq 0$. It is natural to proceed by changing the order of integration which leads to

$$\textbf{(13)}\quad P(\lambda) = \int_{-\infty}^{+\infty} dx \left[\frac{\sin\left(\frac{\pi f}{\sqrt{n}}\right)}{\left(\frac{\pi f}{\sqrt{n}}\right)} \right]^n \int_{\lambda}^{\infty} e^{-j2\pi fx} df$$

and we are left to deal with an inner integral of dubious nature (integration to ∞ of the complex exponential).

The inversion of the characteristic function in this manner has received substantial attention in the literature [3] because this is a frequently encountered computational problem, and several approaches may be used to compute $P(\lambda)$.

A frequent starting point for the inversion of a characteristic function is the Gil-Pelaez theorem [7] that states that the cumulative distribution F(x) can be computed from the characteristic function as

$$\textbf{(14)}\quad F(x) = \frac{1}{2} - \int_{-\infty}^{+\infty} \frac{e^{-j2\pi fx}}{j2\pi f} \phi(f)\,df$$

given the characteristic function $\phi(f)$ [4] where

$$\textbf{(15)}\quad F(x) = \int_{-\infty}^{x} f_x(u)\,du$$

We will make use of this same starting point in the inversion method used here.

If the integration in (14) is approximated by a trapezoidal sum, the Beaulieu series results [5],[6]. As a side note, if n is strictly even in (4), the characteristic function value will be strictly real and positive and the inversion formula may be further simplified to

$$\textbf{(16)}\quad F_{Real}(x) = \frac{1}{2} + \int_{-\infty}^{+\infty} \phi(f) \frac{\sin(2\pi fx)}{2\pi f} df$$

The resulting integral in either form is

nonetheless difficult to evaluate with high precision, particularly for small values of n which lead to extensive tails in the characteristic function $\phi(f)$. The integrand is also difficult to deal with near f=0. If however, (14) is discretized effectively as a discrete Fourier transform (DFT), the very nice closed-form series solution given as

$$\textbf{(17)}\quad F(x) = \frac{1}{2} - \sum_{r=1,Odd}^{\infty} 2\frac{\mathrm{Im}\left[e^{-jr2\pi F_o x}\phi\left(r2\pi F_o\right)\right]}{r\pi}$$

results as reported in [4]. In this series solution, the parameter F_o governs the sampling interval used in the frequency domain, and it should be chosen small compared to the frequency behavior of the characteristic function so that precise results are obtained.

Using this result and the characteristic function derived earlier in (4), we are equipped to investigate the tail probability behavior of the random variable sum for finite n compared to the ideal Gaussian cumulative PDF.

The tail probabilities given as 1-F(x) are computed for a number of different cases in Figure 7 through Figure 12. Depending upon the circumstances involved, these figures provide insight into "how Gaussian" a given situation is when a number n of URVs are being summed. The value xmax that is shown in some of the plots corresponds to the absolute maximum value of x that can occur when summing n URVs as we have been discussing. Mathematically, xmax= (√n) / 2.

Figure 7 Trivial Case n=2

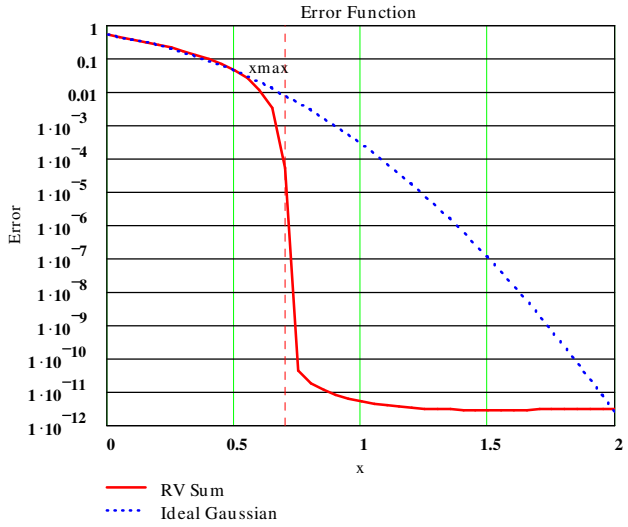

Figure 8 Case n=4

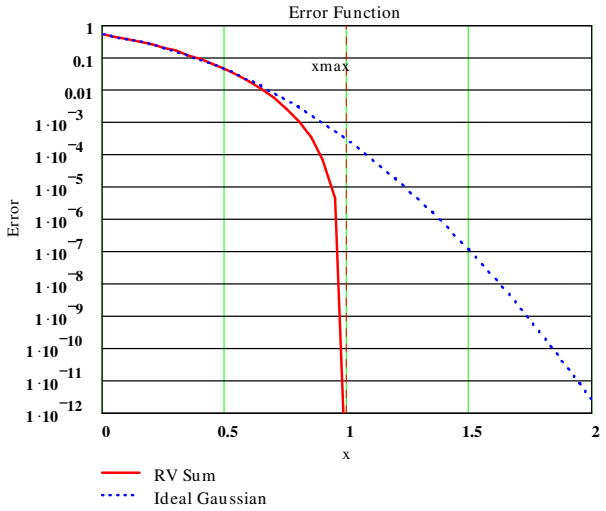

Figure 9 Case n=10

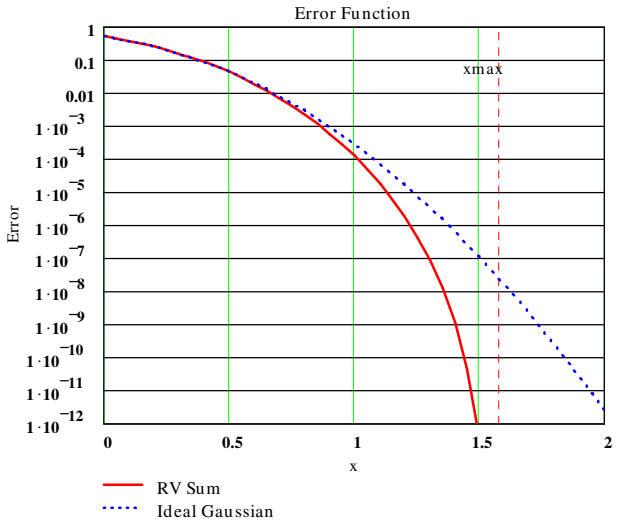

Figure 10 Case n=20

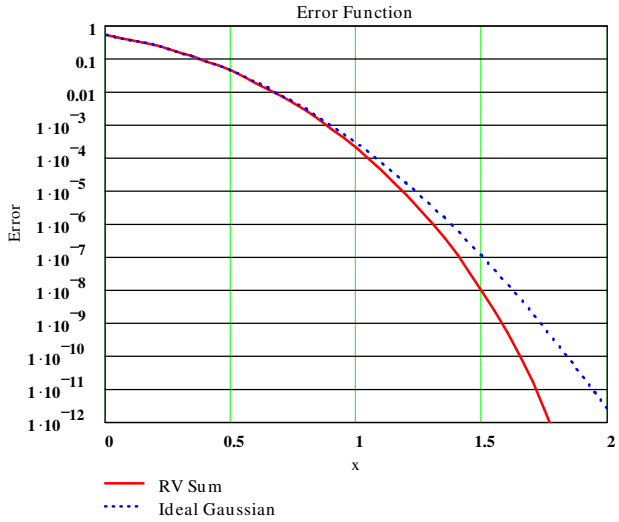

Figure 11 Case n=40

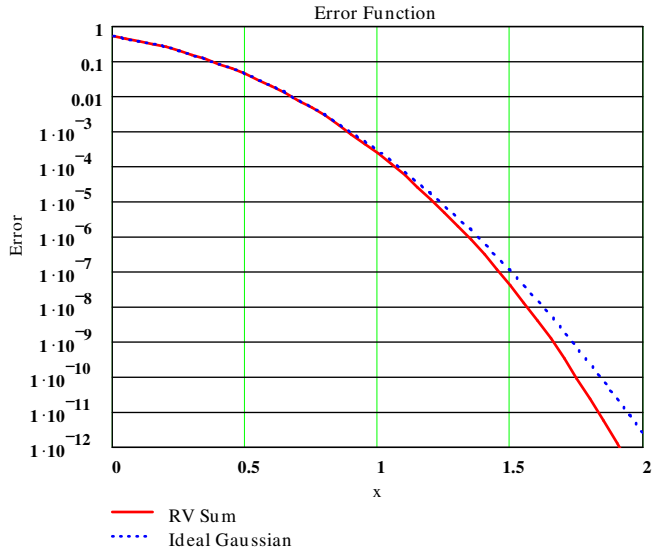

Figure 12 Case n=100

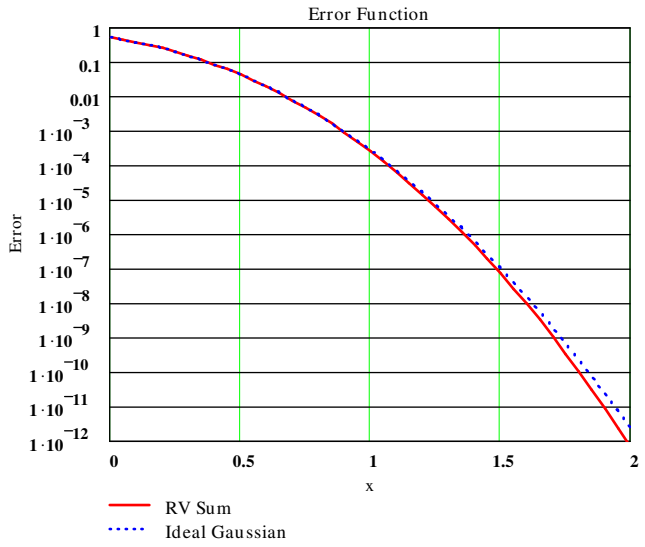

4 Summing Other Types of RVs

Based upon the earlier discussion involving the Central Limit Theorem, we know that summing other types of independent random variables will ultimately lead to a Gaussian distribution also. A more interesting question pertains to how quickly the sum of n such RVs approaches the Gaussian PDF shape, and whether the shape of the underlying PDF has any real significance in the similarity with the Gaussian PDF for finite n.

4.1 Triangular PDF

It seems rather intuitive to first consider this question in the context of a triangular-shaped PDF. The triangular PDF case is particularly interesting because this shape naturally results when two independent URVs are summed. Consequently, we should fully expect that summing n RVs with a triangular PDF will be precisely equivalent to summing 2n URVs. No further work is required to understand how the sum of triangularly distributed RVs will behave.

4.2 Trapezoidal PDF

Consideration of a trapezoidal PDF brings something a little different to bear. However, a trapezoidal PDF corresponds to the PDF that occurs when summing two independent URVs having different variances, so the similarity with our previous results for uniformly distributed RVs will be substantial.

In the case where the two URVs have the PDFs shown in Figure 13 with $\alpha > \beta$, the resulting PDF for the sum of the two RVs will be as shown in Figure 14 with the accompanying characteristic function given as

$$\textbf{(18)}\quad C_{\square}(f) = \left[\frac{1}{2\alpha}\frac{\sin(2\pi\alpha f)}{2\pi\alpha f}\right]\left[\frac{1}{2\beta}\frac{\sin(2\pi\beta f)}{2\pi\beta f}\right]$$

where α and β are arbitrary. Since this case is also very similar to the uniformly distributed case that we have already looked at, it will not be considered further here.

Figure 13 Two Uniformly Distributed RVs with Different Variances

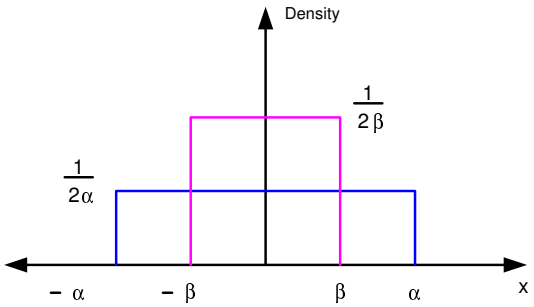

Figure 14 Resultant PDF for Sum of Two Independent Uniformly Distributed RVs with Different Variances

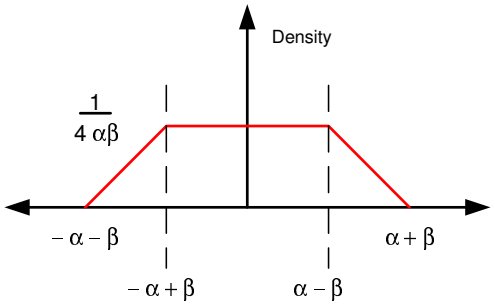

4.3 Parabolic PDF

In this section, we will consider a truly new basic PDF shape as given by

(19) $$f_x(x)=\frac{3}{4}\left(1-x^2\right) \quad for\,|x|\le 1; otherwise\ 0$$

This PDF has the central peak like that of the triangular PDF but is more smooth out to the x-axis endpoints. The variance of this PDF as given by (19) is 1/5. A numerical method for creating parabolically distributed RVs is described in Section 7.4.

A scaling factor must be applied in order to obtain a variance of 1/12 like that which was carried throughout the uniformly distributed RV discussions, and the dependency on the number of RVs summed n must also be added in order to keep the variance of the RV sum constant. Taking these additional factors into account, the appropriate PDF is given by

(20) $$f_x(x,n)=\frac{3\sqrt{n}}{4\alpha}\left[1-\left(\frac{x\sqrt{n}}{\alpha}\right)^2\right] for\ |x|\le\frac{\alpha}{\sqrt{n}};$$
$$otherwise\ 0$$

with $\alpha = \sqrt{(5/12)}$. The characteristic function of the probability density for the sum of n parabolically distributed RV's (PRV) is then given by

$$C_{par}(f,n)=\left[\int_{-\infty}^{+\infty} f_x(x,n)e^{j2\pi fx}dx\right]^n$$

(21)
$$=\left[\int_{-\frac{\alpha}{\sqrt{n}}}^{+\frac{\alpha}{\sqrt{n}}} \frac{3\sqrt{n}}{4\alpha}\left[1-\left(\frac{x\sqrt{n}}{\alpha}\right)^2\right]e^{j2\pi fx}dx\right]^n$$

Since $f_x(\ )$ is an even function of x, the complex exponential within (21) simplifies to a simple cosine. In order to have better numerical accuracy for $C_{par}(f,n)$, use of a closed-form solution for $C_{par}(f,n)$ should be made, and some calculus leads to the respective solution in (22). This characteristic function result can then be used in (17) to compute the underlying PDF of the RV sum. Several example calculations for the sum of parabolic PDF RVs are provided here in Figure 15 through Figure 17.

(22)
$$C_{par}(f,n)=\left\{\frac{3\sqrt{n}}{2\alpha}\left[\frac{\sin\left(\frac{2\pi f\alpha}{\sqrt{n}}\right)}{2\pi f}-\frac{n}{\alpha^2}\left(\frac{\frac{2\alpha}{\sqrt{n}}}{(2\pi f)^2}\cos\left(\frac{2\pi f\alpha}{\sqrt{n}}\right)+\frac{\left(\frac{2\pi f\alpha}{\sqrt{n}}\right)^2-2}{(2\pi f\alpha)^3}\sin\left(\frac{2\pi f\alpha}{\sqrt{n}}\right)\right)\right]\right\}^n$$

Figure 15 Parabolic Distributed RV Sum n=4

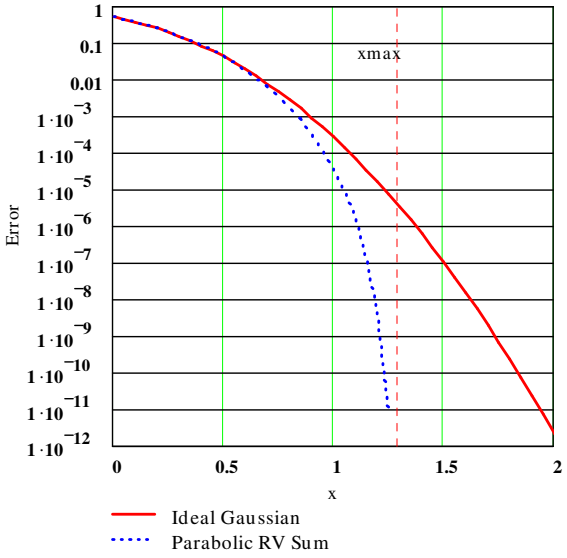

Figure 16 Parabolic Distributed RV Sum n=20

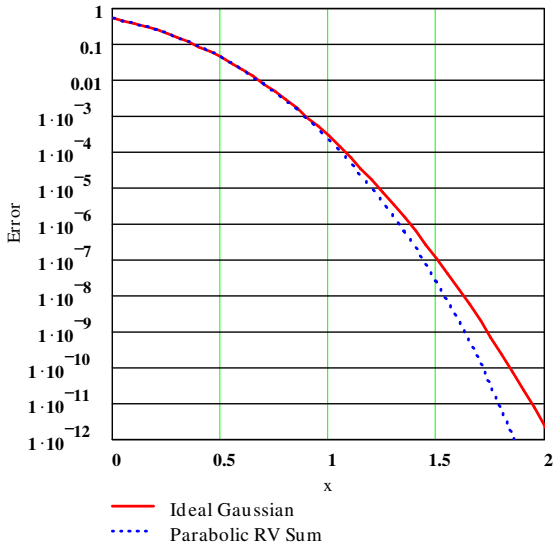

Figure 17 Parabolic Distributed RV Sum n=40

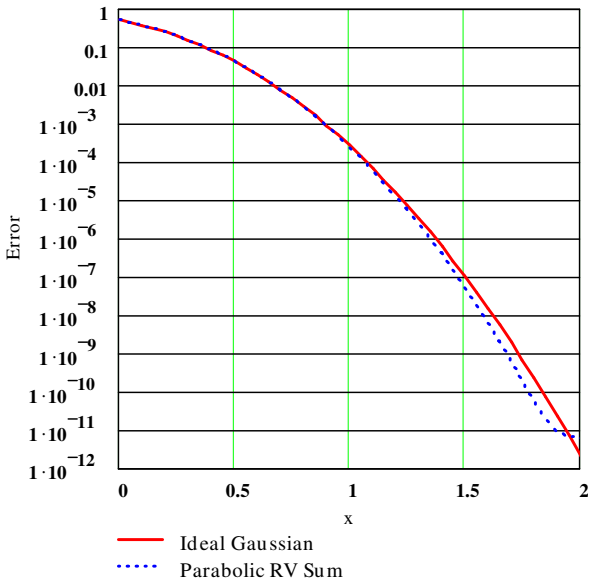

A casual comparison of these results with those of the uniformly distributed case reveal that the parabolic RV sums are somewhat more faithful in producing the near-Gaussian PDF characteristic for n < 40. The differences are not substantial however, except for very small n. Once again, we see that the onset of the Central Limit Theorem supercedes the shape of the underlying individual RV PDF substantially.

5 Application

Years ago before processors and digital signal processing were far less powerful than they are today, creating a Gaussian random variable was not necessarily a trivial matter. The temptation to do something as simple as adding URVs together to address this issue was always lurking. Highly accurate creation of Gaussian RVs otherwise involves a logarithmic and square-root function as shown later in this section.

In more recent times, the most prevalent manner for generating quality Gaussian RVs is to make use of the Box-Muller algorithm in conjunction with multiple linear congruence generators that create a high-quality uniformly distributed RV. The Wickmann-Hill algorithm is often cited regarding the creation of high-quality uniformly distributed RVs.

The Box-Muller algorithm is based upon starting with a 2-dimensional Gaussian PDF and converting it into polar form.

$$f_{x,y}(x,y) = \frac{1}{\sigma_x\sqrt{2\pi}} e^{-\frac{x^2}{2\sigma_x^2}} \frac{1}{\sigma_y\sqrt{2\pi}} e^{-\frac{y^2}{2\sigma_y^2}}$$

(23)

$$= \frac{1}{2\pi\sigma_x\sigma_y} e^{-\frac{1}{2}\left(\frac{x^2}{\sigma_x^2}+\frac{y^2}{\sigma_y^2}\right)}$$

In the case where we take the variances of x and y to be identically equal to σ^2, this simplifies further to

(24) $$f_{x,y}(x,y) = \frac{1}{2\pi\sigma^2} e^{-\frac{1}{2\sigma^2}\left(x^2+y^2\right)}$$

It is straight forward to convert this 2-dimensional PDF to polar form as[1]

(25) $$f_{r,\theta}(r,\theta) = \frac{r}{2\pi\sigma^2} e^{-\frac{1}{2}\left(\frac{r}{\sigma}\right)^2}$$

where $r = \sqrt{(x^2 + y^2)}$ and $\theta = \text{atan}(y,x)$. If we further integrate out the uniformly distributed parameter θ, we are left with the well-known Rayleigh distribution and it is a simple matter to compute the cumulative probability function for the Rayleigh case as

(26) $$P(\lambda) = \int_{\lambda}^{\infty} \frac{r}{\sigma^2} e^{-\frac{1}{2}\left(\frac{r}{\sigma}\right)^2} dr = e^{-\frac{1}{2}\left(\frac{\lambda}{\sigma}\right)^2}$$

This result can be easily transformed into a form that makes it possible to create Rayleigh RVs from a uniformly distributed RV since we may write

(27) $$\lambda = \sqrt{-2\sigma^2 ln\left[P(\lambda)\right]}$$

This is the same formula used in the Box-Muller Gaussian RV algorithm with P(λ) replaced by a uniform random number generator spanning (0,1]. Once equipped with the Rayleigh-distributed RV λ, it is a simple matter to augment this with the uniformly distributed phase θ over (0,2π] and form two independent Gaussian RVs as

[1] θ is uniformly distributed over 2π and does not explicitly show up in this equation. Integration with respect to θ would eventually be involved at some point.

$$\text{(28)} \quad \begin{aligned} g_1 &= \lambda\cos(\theta) \\ g_2 &= \lambda\sin(\theta) \end{aligned}$$

Some of the results presented herein may also provide some insight into physical problems where a finite number of RVs are effectively added together during some process. Expansion of the concepts developed here can shed insight into whether or not the underlying process may be assumed to be Gaussian or not, and what kind of ensuing errors may follow if the Gaussian assumption is nevertheless made.

Computation of bit error rate (BER) for a bit synchronizer or digital communication system often entails inversion of a characteristic function if an analytical solution is pursued. In the case of a bit synchronizer, it is common place to look at BER in the presence of Gaussian noise and intersymbol interference (ISI). The characteristic function for the Gaussian noise is known whereas the characteristic function for the ISI must be found. If the probability of data-ones and data-zeros are equal, and the noise-free output signal shape for an individual data symbol can be represented by g(t) in which t=0 corresponds to the steady-state sampling point for the symbol, it can be shown that the characteristic function for the ISI is given by [8],[9]

$$\text{(29)} \quad C_{ISI}(f) = \prod_{\substack{e=-\infty \\ e\neq 0}}^{+\infty} \cos\left[2\pi f g(eT)\right]$$

The characteristic function of the Gaussian noise plus ISI is then simply the product of the two characteristic functions, and (17) may be used to evaluate the BER in the case of hard decisions.

Any practicing engineer who works with random quantities should be certain to add the Box-Muller algorithm to their toolbox if not already present. The inversion formula given by (17) in Section 3.1 and (31) in Section 7.3 should be equally tucked away for future use.

6 References

1. Jaynes, E.T., ***Probability Theory: The Logic of Science***, Cambridge University Press, 2003
2. Papoulis, A., ***Probability, Random Variables, and Stochastic Processes***, McGraw-Hill Book Co., 1965
3. Abate, J., Whitt, W., "The Fourier Series Method for Inverting Transforms of Probability Distributions", 19 September 1991
4. Tellambura, C., Annamalai, A., "Further Results on the Beaulieu Series", IEEE Trans. Communications, Nov. 2000
5. Beaulieu, N., "An Infinite Series for the Computation of the Complementary Probability Distribution Function of a Sum of Independent Random Variables and Its Application to the Sum of Rayleigh Random Variables", IEEE Trans. Communications, Sept. 1990
6. Beaulieu, N., "The Evaluation of Error Probabilities for Intersymbol and Cochannel Interference", IEEE Trans. Communications, Dec. 1991
7. Gil-Pelaez, J., "Note on the Inversion Theorem", Biometrika, vol. 38, pp. 481-482, 1951
8. Crawford, J.A., "Cair Bit Synchronizer", U11592, 1990, page 27 (This Website)
9. _____, "Bit Synchronizer Talk", 1988, U11589, page 16 (This Website)

7 Appendix: Notes

7.1 Characteristic Functions

The characteristic function is an indispensable tool in some areas of probability theory. One of these areas involves the sum of IRVs because the PDF of the sum is given by a convolution of the individual PDFs involved. Since it is far easier to work with an n-fold product of Fourier transforms than to do n convolutions, the Fourier-based characteristic function approach is much preferred.

The characteristic function of a PDF $f_x(x)$ is given by definition as

$$\text{(30)} \quad C_x(f) = \int_{-\infty}^{+\infty} f_x(x) e^{j2\pi fx} dx$$

The inverse Fourier transform is used to compute the underlying PDF from a given characteristic function.

We make use of the characteristic function in primarily two ways within this memorandum. In the first manner, we use it to replace the n-dimension convolution that would result from summing n IRVs with a much easier n-fold multiplication of characteristic functions. In the second manner, we make use of the one-to-one correspondence between a PDF and its characteristic function in order to show that in the limit as $n \to \infty$, the IRV sum does in fact become a Gaussian PDF. This conclusion follows from recognizing that the underlying characteristic function as $n \to \infty$ is shown to equal the characteristic function

of a Gaussian RV.

In general, characteristic functions are invaluable when dealing with IRV involving sums as well as moments. The interested reader is encouraged to consult [2] for additional details.

7.2 Cumulative PDF Characteristic Function

From transform theory, we know that if a probability density function $f_x(x)$ has a characteristic function $\phi_x(f)$, the transform of the cumulative probability function $F_x(t)$ is given by[2] $\phi_x(f) / (-j2\pi f)$. This may be substantiated by noting that

$$\begin{aligned} f_x(t) &= \lim_{\delta\to 0}\frac{F_x(t+\delta)-F_x(t)}{\delta} \\ &= \lim_{\delta\to 0}\int_{-\infty}^{+\infty}\frac{\phi_x(f)}{-j2\pi f}\left[\frac{e^{-j2\pi f(t+\delta)}-e^{-j2\pi ft}}{\delta}\right]df \\ &= \lim_{\delta\to 0}\int_{-\infty}^{+\infty}\phi_x(f)e^{-j2\pi f(t-\delta/2)}\left(\frac{e^{-j\pi f\delta}-e^{j\pi f\delta}}{-\delta j2\pi f}\right)df \\ &= \lim_{\delta\to 0}\int_{-\infty}^{+\infty}\phi_x(f)e^{-j2\pi f(t+\delta/2)}\left(\frac{\sin(\pi f\delta)}{\pi f\delta}\right)df \\ &= \int_{-\infty}^{+\infty}\phi_x(f)e^{-j2\pi ft}df \end{aligned}$$

7.3 Inversion of Characteristic Functions

A formula similar to (17) is available for the inversion of a characteristic function to its respective probability density function [4]. The utility of this series-style solution should not be underestimated, and it is therefore included in this appendix for that reason.

(31) $$f_x(x) = 4F_o\sum_{r=1,Odd}^{\infty}\mathrm{Re}\left[e^{-jr2\pi F_o x}\phi\left(r2\pi F_o\right)\right]$$

[2] The negative sign is due to the definition of the characteristic function transform which uses a complex exponential kernel function of exp(j2πfx) which is slightly different than for the forward Fourier transform.

7.4 Creating Parabolically Distributed RVs

The creation of parabolically distributed RVs is offered here without proof based upon some of the techniques employed in Section 5. Assume that F is a URV distributed on the range (0,1]. The corresponding PRV which should be mapped to this value of F is the solution x to the equation

(32) $$g(x) = x^3 - 3x + 4F - 2 = 0$$

Although inefficient for practical implementations, the Newton-Raphson technique can be used to solve (32) using the iterative formula

(33) $$x_{k+1} = x_k - \frac{g(x_k)}{3x_k - 3}$$

with $x_0 = 0$ and $k \in [0,10]$. The returned PRV is given by x_{10} for each value of F.

7.5 Unsuitable PDFs

Not all RV PDFs are suitable for summing in the manner discussed in this paper. Take for instance the rational PDF given as

(34) $$f_x(x) = \frac{a}{\pi}\frac{1}{a^2+x^2}$$

The total probability for this choice of PDF is unity as required, but the variance of the underlying PDF is unbounded. In general, the exponent of x in the denominator must exceed the exponent of any x-term in the numerator by more than 2 in order to avoid this problem.

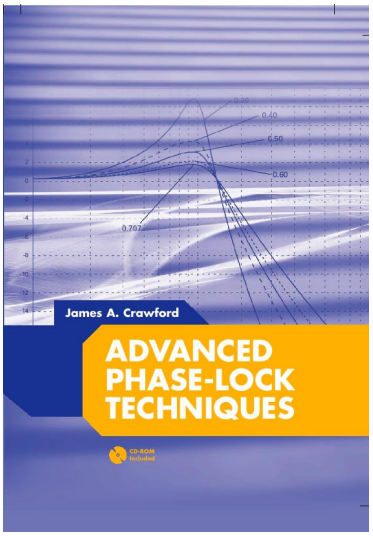

Advanced Phase-Lock Techniques

James A. Crawford

2008

Artech House

510 pages, 480 figures, 1200 equations
CD-ROM with all MATLAB scripts

ISBN-13: 978-1-59693-140-4
ISBN-10: 1-59693-140-X

Chapter	Brief Description	*Pages*
1	*Phase-Locked Systems—A High-Level Perspective* An expansive, multi-disciplined view of the PLL, its history, and its wide application.	26
2	*Design Notes* A compilation of design notes and formulas that are developed in details separately in the text. Includes an exhaustive list of closed-form results for the classic type-2 PLL, many of which have not been published before.	44
3	*Fundamental Limits* A detailed discussion of the many fundamental limits that PLL designers may have to be attentive to or else never achieve their lofty performance objectives, e.g., Paley-Wiener Criterion, Poisson Sum, Time-Bandwidth Product.	38
4	*Noise in PLL-Based Systems* An extensive look at noise, its sources, and its modeling in PLL systems. Includes special attention to 1/*f* noise, and the creation of custom noise sources that exhibit specific power spectral densities.	66
5	*System Performance* A detailed look at phase noise and clock-jitter, and their effects on system performance. Attention given to transmitters, receivers, and specific signaling waveforms like OFDM, M-QAM, M-PSK. Relationships between EVM and image suppression are presented for the first time. The effect of phase noise on channel capacity and channel cutoff rate are also developed.	48
6	*Fundamental Concepts for Continuous-Time Systems* A thorough examination of the classical continuous-time PLL up through 4^{th}-order. The powerful Haggai constant phase-margin architecture is presented along with the type-3 PLL. Pseudo-continuous PLL systems (the most common PLL type in use today) are examined rigorously. Transient response calculation methods, 9 in total, are discussed in detail.	71
7	*Fundamental Concepts for Sampled-Data Control Systems* A thorough discussion of sampling effects in continuous-time systems is developed in terms of the *z*-transform, and closed-form results given through 4^{th}-order.	32
8	*Fractional-N Frequency Synthesizers* A historic look at the fractional-N frequency synthesis method based on the U.S. patent record is first presented, followed by a thorough treatment of the concept based on Δ-Σ methods.	54
9	*Oscillators* An exhaustive look at oscillator fundamentals, configurations, and their use in PLL systems.	62
10	*Clock and Data Recovery* Bit synchronization and clock recovery are developed in rigorous terms and compared to the theoretical performance attainable as dictated by the Cramer-Rao bound.	52